Piezoelectrically Actuated Miniature Peristaltic Pump

Yoseph Bar-Cohen and Zensheu Chang

Jet Propulsion Laboratory (JPL)/Caltech[1]

ABSTRACT

There is a range of NASA experiments, instruments and applications where miniature pumps are needed. To address such needs, a piezoelectrically actuated miniature pump is being developed. This pump employs a novel volume displacing mechanism using flexural traveling waves that acts peristaltically and eliminates the need for valves or physically moving parts. This pump is being developed for planetary instruments and space applications. Finite element model was developed using ANSYS for the purpose of prediction of the resonance frequency of the vibrating mode for the piezo-pump driving stator. The model allows determining simultaneously the mode shapes that are associated with the various resonance frequencies. This capability is essential for designing the pump size and geometry. To predict and optimize the pump efficiency that is determined by the volume of pumping chambers the model was modified to perform harmonic analysis. Current capability allows the determination of the effect of such design parameters as pump geometry, construction materials and operating modes on the volume of the chambers that are formed between the peaks and valleys of the waves. Experiments were made using a breadboard of the pump and showed water-pumping rate of about 4.5 cc/min. The pump is continually being modified to enhance the performance and efficiency.

Keywords: Pumps, piezoelectric actuation, piezopump, peristaltic pump, actuators

1. INTRODUCTION

NASA's mission requirements are becoming more stringent in terms of mass, dimensions, power and cost with a growing emphasis on the reliability of planetary instruments and spacecraft subsystems. These constraints are determining the type of instruments and devices that will be used in future missions and they are impacting the requirements for pumps that can be employed. Pumps are used for a wide variety of applications including thermal management, cooling systems, mass spectrometers, vacuum-controlled devices, and compressors. NASA is increasingly becoming involved with planet surface sampling missions and *in-situ* remote analysis where there is a need to enable movement of liquids in instrumentation. The pumps are required to transport liquids, which potentially contain bacteria and other microorganisms, through filter media and the displaced volume can be as low as milliliters.

Pumps [Weissler and Carlson, 1979; Lucovsky, 1989] with moving parts have critical seal problems, tend to wear relatively quick, require a relatively high power, exhibit a number of reliability problems, are difficult to miniaturize and have limited temperature performance. To address these issues, a study is currently underway at the Jet Propulsion Laboratory's NDEAA Technologies Lab to develop a piezoelectrically actuated miniature pump (so-called piezopump) that can overcome the limitations of conventional mechanisms. Piezopump is being developed as a miniature low power device. A novel volume displacing mechanism using flexural traveling waves, which acts peristaltically and allows the elimination of the need for valves or physically moving parts, induces the pumping effect. The pumping action is obtained by employing the multiple chambers that are formed between peaks and valleys of the traveling wave. The foundations for the development of a piezoelectrically driven pump were laid under the NASA task, entitled "Planetary Dexterous Manipulator", where piezoelectric motors have been developed as an alternative to conventional electric motors [Lih and Bar-Cohen, 1997]. Generally, piezoelectric motors have unique characteristics that are attractive to robotic applications [Hollerbach, Hunter and Ballantyne, 1991; Hagood and McFarland, 1994] including miniaturization, low power consumption, self-holding force and simple construction. With proper electronics' logic (compensating for the effect of temperature on the piezoelectric coefficients), recent experiments at JPL have shown that these motors work effectively at temperatures of 120K and vacuum of 16-mTorr with a torque-speed performance similar to room temperature [Bar-Cohen, Bao, and Grandia, 1998]. The characteristics of ultrasonic motors allows developing piezopumps that do not need valves, exhibit low backflow and have the potential of high reliable since no physically moving parts are involved. In order to maximize the pump efficiency, a

---

[1] Correspondence: JPL, (MS 82-105), 4800 Oak Grove Drive, Pasadena, CA 91109-8099 Email yosi@jpl.nasa.gov; web: http://ndea.jpl.nasa.gov

parametric study (fluid and solid mechanics, thermal) is underway and the results of this study will be reviewed in this manuscript.

2. TRAVELING WAVES AS AN ACTUATION MECHANISM

In the past few years, piezoelectric materials have seen a surge in use for actuators such as rotary motors, inchworms and other drive mechanisms. Ultrasonic motors have emerged on Japanese commercial products such as auto-focus cameras. These piezoelectric motors offer potential advantages in the areas of power efficiency, torque/mass ratios, compact size, and efficient self-holding force [Hagood and McFarland, 1994]. This motor technology provides the basis for a piezoelectric pumping mechanism that can be used to transfer liquids between media. To assist in understanding the pumping mechanism, the piezoelectric motor technology is reviewed briefly in the following paragraphs.

Piezoelectric motors [Lih and Bar-Cohen, 1997; Hollerbach, Hunter and Ballantyne, 1991; Hagood and McFarland, 1994] are driven by microscopic material deformations that are amplified through either quasi-static mechanical or dynamic/resonant means. Piezoelectric motors have seen commercial application in areas needing compact, efficient, intermittent motion. Such applications include camera auto focus lenses [Hosoe, 1989], watch motors [Seiko instruments Inc., 1992] and compact paper handling [Inoue, Takahashi and Saga, 1989]. In Figure 1, the operation principle of a piezoelectric motor is shown, where a stator, actuated by piezoelectric crystals, propels a rotor that is in intimate contact with it. A traveling flexural wave is established over the surface of the elastic stator that propels the rotor pressed onto it using the elliptical particle motion. This operation of piezoelectric motors depends on friction at the interface between the stator and rotor.

Reviewing the operation principal of the piezoelectric motor, it is easy to see the formation of multiple chambers between the crests of the traveling wave. These chambers offer a platform for the transportation of captured gas or fluid in the direction of the wave propagation. The operation principle of our piezopump is based on using these multiple chambers, as shown schematically in Figure 2. To illustrate the pumping action, one can design a pump based on two synchronized back-to-back stators that serve as stationary drive elements that are excited individually by piezoelectric actuators. The wave travels synchronously at the interface and forms multiple chambers that are filled with the desired gas or liquid. The chambers are formed, closed and travel in a rolling motion that can be described as a squeezing effect. This peristaltic synchronized action of the wave is not associated with any physically moving parts and is a frictionless wave travel movement.
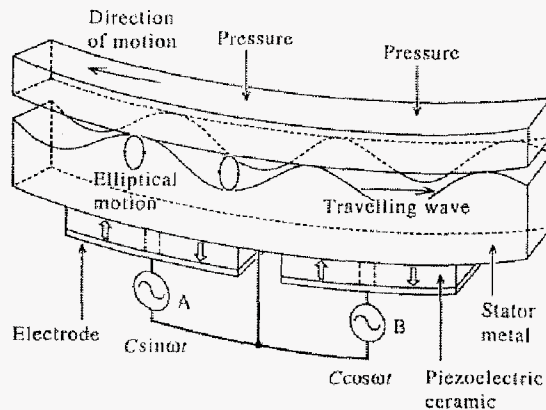

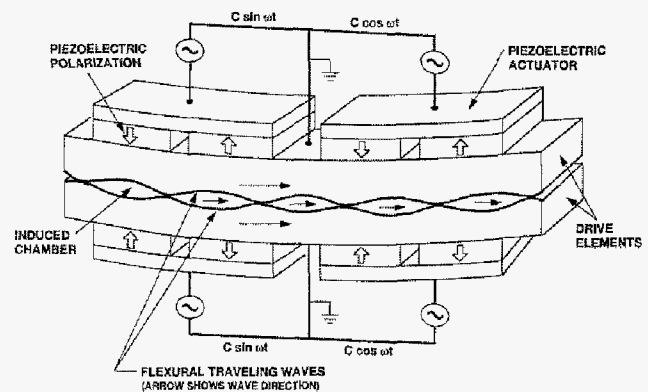FIGURE 1: Principle of operation of a piezoelectric motor.

FIGURE 2: Principle of operation of the proposed piezoelectric pump

The opening of each moving chamber between the two stators defines the dimensions of the chambers. An important feature of piezopump is its elimination of the need for valves, sliding seals or other components that can cause wear. The pumped fluids or gases are flowing along the traveling wave direction. The multiple chambers are formed between the two synchronously actuated stators that are pressed against each other (typically held at a pressure level of at least 1-2 ksi) to produce a tightly sealed interface. These tight surfaces of the pump shut the flow when the pump is turned off, producing a self-locking effect with the characteristics of a valve.

The modeling of the stator, which serves as the basis for developing the piezopump, has been very successful and an excellent agreement was observed between the mode characteristics as corroborated experimentally by an interferometric

setup at MIT (see Figure 3). Also, modal analysis showed an excellent agreement between the measured and calculated resonance frequency of the stator.
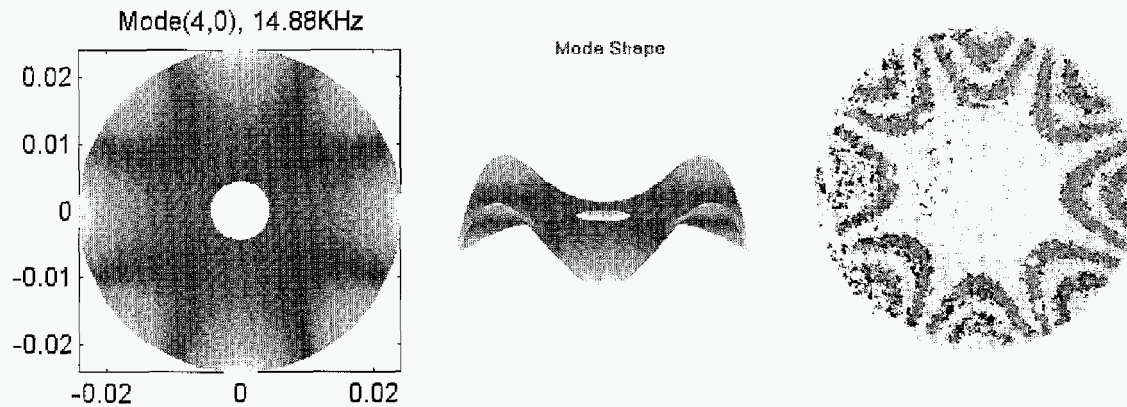
Mode(4,0), 14.88KHz

Mode Shape

FIGURE 3: A view of the theoretical prediction of the frequency response of a stator that is driven by 4-mode piezoelectric actuators (left) and the experimental corroboration using interferometry.

A finite element model was developed using the results of the modeling of ultrasonic motors and it accounts for the key components of the pump, i.e. stators, interface, and piezoelectric actuators. Experiments were conducted to corroborate the predications of the model.

3. MODELING PIEZOPUMP

The stator is modeled as a plate that is subjected to distributed piezoelectric forces as well as distributed normal and tangential interface pressures caused by the stators at the contact points. To allow the consideration of distributed normal and tangential forces in the model, the model will include traveling wave motion through temporally and spatially out-of-phase forcing of 90° orthogonal wave modes. The contact points of the stators at the interface will be assumed as compliant. The pump performance is predicted using transient and steady state values of the actuation elements to calculate the pumping efficiency.

The selected materials and configuration of the pump determine its efficiency and ability to operate effectively at low ambient pressures and temperatures such as the environment of Mars. The analytical model incorporated parameters that affect the operation of the pumps in space environment and provide a guide in the selection of the critical materials for the construction of the pump (actuation elements, stator material, surface coating, etc.). The flexural traveling wave is induced by PZT-4d that is known as effective piezoelectric actuators with a high d_{31} flexure coefficient allowing to induce large wave amplitudes. Initially, we concentrated on establishing the preliminary finite element model and the demonstration of the feasibility of the novel concept of the piezopump using flexural traveling waves as a pumping mechanism. We constructed a brassboard pump and demonstrated that water can be peristaltically pumped over a distance of one wavelength. Later, we studied the operation of piezopumps with stator that is made of stainless steel, bronze, or aluminum.

We created a finite element model using ANSYS for the prediction of the resonance frequency of the vibrating mode for the piezopump metal ring. The first model featured a portion of the metal ring, and it gave us only the resonance frequency of a specific mode. Our experiments have shown that it is essential to keep the resonance frequency of the desired mode away from adjacent modes. This requirement led us to modifying the model to allow simultaneous derivation of the resonance frequencies at various modes. Figure 4 shows a typical mesh for the finite element analysis. This capability is also essential to the determining and designing of pump size and geometry. Figure 5 shows a typical ANSYS result of the resonance frequency analysis.
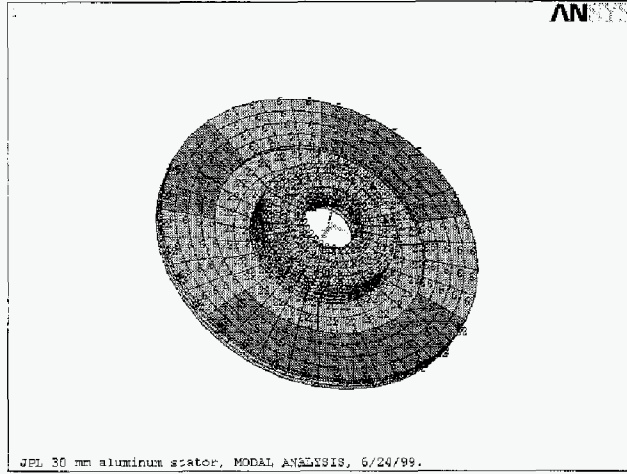
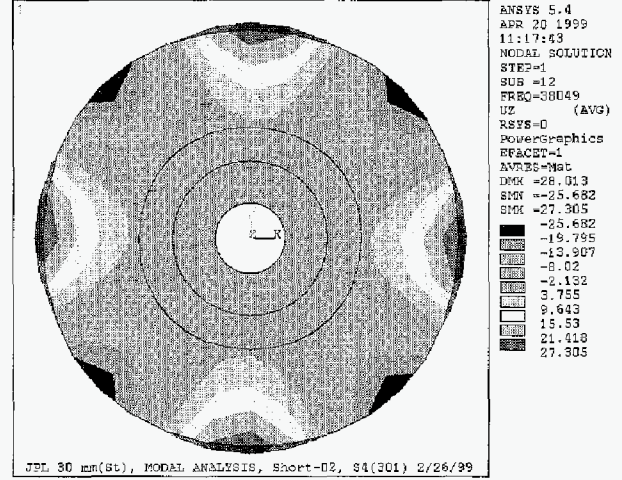**Figure 4**: A typical mesh for the finite element analysis.

Figure 5: An ANSYS result of the resonance frequency analysis for a piezo-pump ring.

In finite element analysis, the equation of motion for an undamped system, expressed in matrix notation is:

$$[M]\left\{\ddot{u}\right\}+[K]\{u\}=\{0\} \tag{1}$$

where: [M] - structural mass matrix.
   [K] - structural stiffness matrix.
   {u} - nodal displacement vector.
   The dot symbol means derivative with respect to time.

For a linear system, free vibration will be harmonic of the form:

$$\{u\}=\left\{\phi\right\}_{i}\cos\omega_{i}t \tag{2}$$

where: $\{\phi\}_i$ - eigenvector representing the mode shape of the ith resonance frequency.
   ω_i - i^{th} resonance circular frequency (radians per second).
   t - time.

Substitute Equation (2) into (1), we have:

$$\left(-\omega_i^2[M]+[K]\right)\{\phi\}_i=\{0\} \tag{3}$$

To derive nontrivial solutions, the determinant of ([K] - ω^2[M]) must be zero. So we have:

$$\left|[K]-\omega^2[M]\right|=0 \tag{4}$$

This is an eigenvalue problem which may be solved for up to n values resonance frequencies and eigenvectors that satisfy Equation (3), where n is the number of Degree Of Freedoms (DOFs). The results of the resonance frequency analysis are shown in the next section together with the experiment results.

Since it was determined that the prediction of the pump efficiency requires determination of the induced chambers during operation, it was necessary to modify the finite element model further. Using ANSYS, efforts were initiated to conduct harmonic analysis of the piezopump. Consider the general equation of motion for a structural system:

$$[M]\left\{\ddot{u}\right\}+[C]\left\{\dot{u}\right\}+[K]\{u\}=\{F\} \tag{5}$$

where: [C] = structural damping matrix.
   {F} = applied load vector.

All points in the structure are moving at the same known frequency, however, not necessarily in phase. Also, it is known that the presence of damping causes phase shifts. Therefore, the displacements may be defined as:

$$\{u\} = \left\{u_{\max} e^{i\phi}\right\} e^{i\Omega t} \tag{6}$$

where: $u_{\max}$ = maximum displacement.
   i = the imaginary number (square root of –1).
   Ω = imposed circular frequency.
   ϕ = displacement phase shift.

The use of complex notation allows a compact and efficient description and solution of the problem. Equation (6) can be rewritten as:

$$\{u\} = \left(\{u_1\} + i\{u_2\}\right) e^{i\Omega t} \tag{7}$$

where: $\{u_1\} = \{u_{max} \cos \phi\}$
   $\{u_2\} = \{u_{max} \sin \phi\}$

The force vector can be specified analogously to the displacement:

$$\{F\} = \left(\{F_1\} + i\{F_2\}\right) e^{i\Omega t} \tag{8}$$

Substitute Equations (7) and (8) into Equation (5), we have:

$$\left([K] - \Omega^2[M] + i\Omega[C]\right)\left(\{u_1\} + i\{u_2\}\right) = \left(\{F_1\} + i\{F_2\}\right) \tag{9}$$

The methods used to solve Equation (9) is the same as those used to solve a static problem, except that it is done using complex arithmetic.

Parametric study of the piezopump had been done on the driving mode and the material of the stator. Details can be found in our previous paper [Bar-Cohen and Chang, 2000]. The relationship between the thickness of the piezoelectric ring and the performance of the piezopump was studied and shown here. Effective coupling factors K were calculated for piezopumps with piezoelectric rings of different thickness. Basically, the effective coupling factor K indicates how much energy is stored mechanically in a piezoelectric device when it is activated. Higher value of the factor usually means better efficiency of the device. By investigating the effective coupling factors of pumps with piezoelectric rings of different thickness, it is expected that an optimal thickness can be found, and thus the performance of the piezopump can be improved.

$$K = \sqrt{1 - \frac{f_r^2}{f_a^2}} \tag{10}$$

where f_r is the resonance frequency, and f_a is the anti-resonance frequency of the device. Both the resonance and the anti-resonance frequencies are derived from ANSYS's modal analysis with proper boundary conditions. Figure 6 shows the effective coupling factor vs. the ratio of the thickness of piezoelectric ring to the total thickness of the stator. Maximum K occurs where the thickness ratio is equal to about 0.4.

We had tried two different thickness ratio, 0.25 and 0.35. The pumping rate for ratio 0.25 is 1.5 cc per minute, and for ratio 0.35 is 4.5 cc per minute.
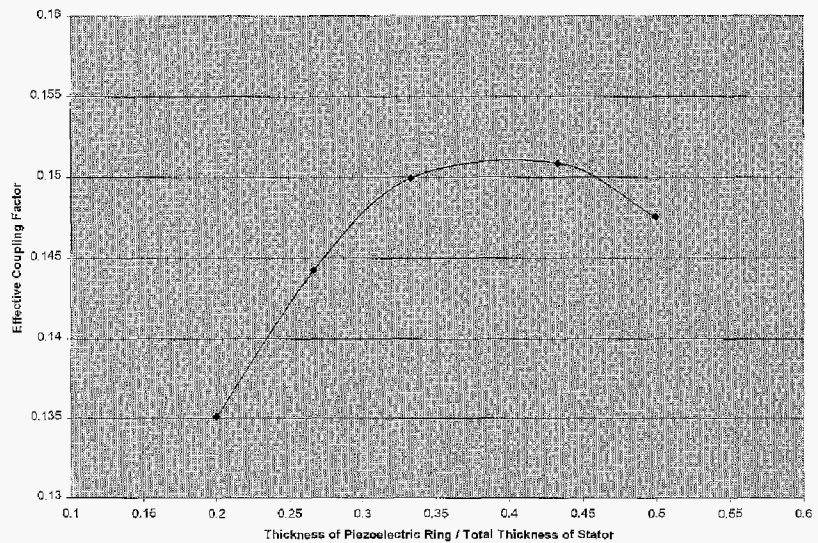

Figure 6: Effective coupling factor vs. Thickness ratio.

4. EXPERIMENTS

Based on the novel volume displacing mechanism using elastic traveling wave, and results of the finite element modeling, we designed and fabricated a pump stator and a Plexiglas seal plate. A piezoelectric ring was bonded to the metal ring to form the pump drive stator, a plastic fluid guide and silicon rubber were used to channel the fluid within the pump chambers. Figure 7 shows cross section and side view sketches of the metal ring. Figure 8 shows a sketch of the piezoelectric ring with the polarity sequence as designed to activate 4-wave mode. Figure 9 shows the components of the piezopump brassboard and Figure 10 shows the components of the pump.
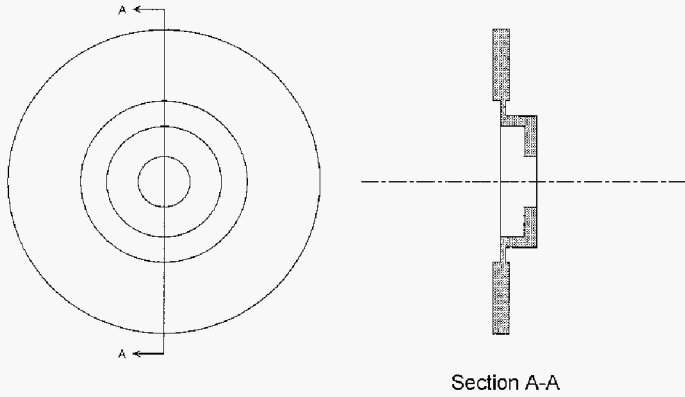

Section A-A

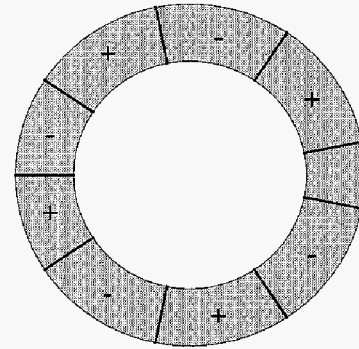**Figure 7**: Metal ring of the piezo pump.

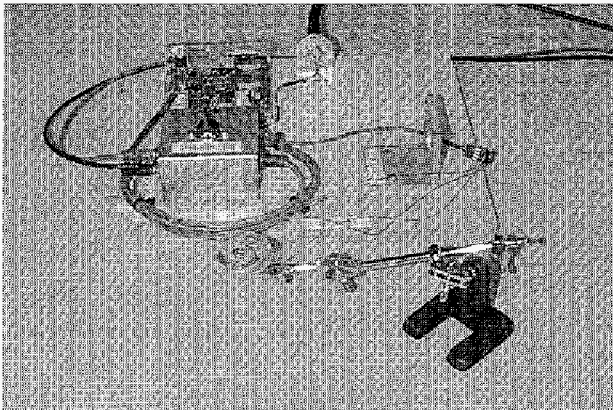**Figure 8**: A piezoelectric ring designed for 4-wave mode.
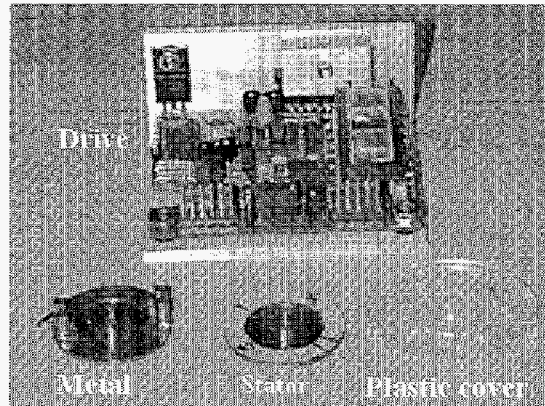

Figure 9: Piezopump brassboard system.

Figure 10: Components of a piezopump.

As shown in Figure 8, the silver electrode on the piezoelectric ring is divided into several sections. Each section is polarized either positive or negative. The one section not polarized is used as a transducer (i.e., sensor) for collecting feed back data. The polarized piezoelectric ring is bonded to the metal ring of the stator using epoxy. A plastic cover with tubes attached is then mounted on the other surface of the metal ring using silicon rubber. The assembled pump was tested electrically using an Impedance/Gain-Phase Analyzer (Schlumberger, SI 1260) to experimentally determine the resonance frequency. Figure 11 shows a typical result of the impedance analysis. The peak in the phase angle chart identifies the resonance frequency for the mode under investigation. The resonance frequencies derived from these tests are shown in Table 3 together with the associated theoretical results and the error percentage. The largest error percentage that was measured between the predictions and the
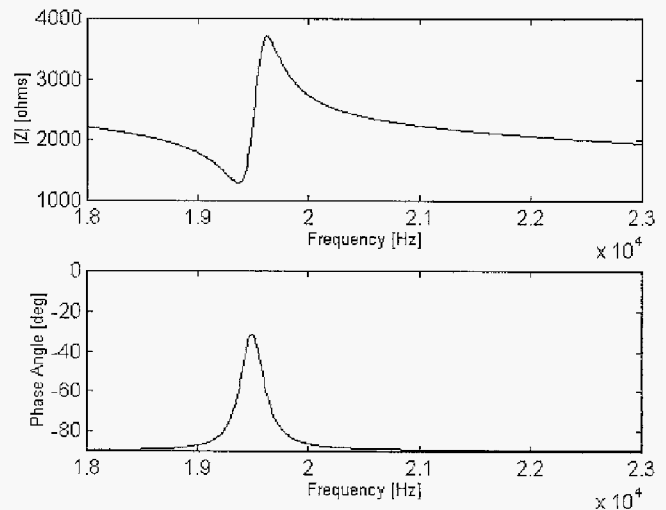

Figure 11: An impedance test result.

experimental data is 9.9 percent, while the smallest one is 0.9 percent. It was noted that usually higher modes show larger discrepancy between theoretical and experimental results. This is probably because we used elements with similar size for all the different modes. So the accuracy of the theoretical results for higher modes is not as good as for lower modes.

TABLE 3: Comparison of theoretical and experimental results of resonance frequency.

Mode	Stainless Steel			Aluminum			Bronze		
	ANSYS	Test	Error	ANSYS	Test	Error	ANSYS	Test	Error
3-Wave	15.3	14.9	2.6%	14.4	14.7	2.1%	11.7	11.8	0.9%
4-Wave	27.3	25.6	6.2%	26.1	25.8	1.1%	21.1	20.5	2.8%
5-Wave	43.3	39.0	9.9%	41.7	39.4	5.5%	33.7	32.3	4.2%

Figure 12 shows from two different angles of views for a working pump while pumping water. All the assembled pumps were measured for their performance in terms of pumping rate and the highest pressure that the pump can reach. The pumping rate of the pump was measured by collecting the water that is pumped in 1 minute. The volume of the collected water was then measured using a graduated cylinder. The highest pressure the pump can reach is measured by pumping water into a vertical tube. The highest level that the water reached represents the highest pressure the pump can sustain. So far, the best performance that was recorded is about 4.5 cc/min in pumping rate, and the highest water level reached is about 11 cm, which is equal to about 1100 Pascal.
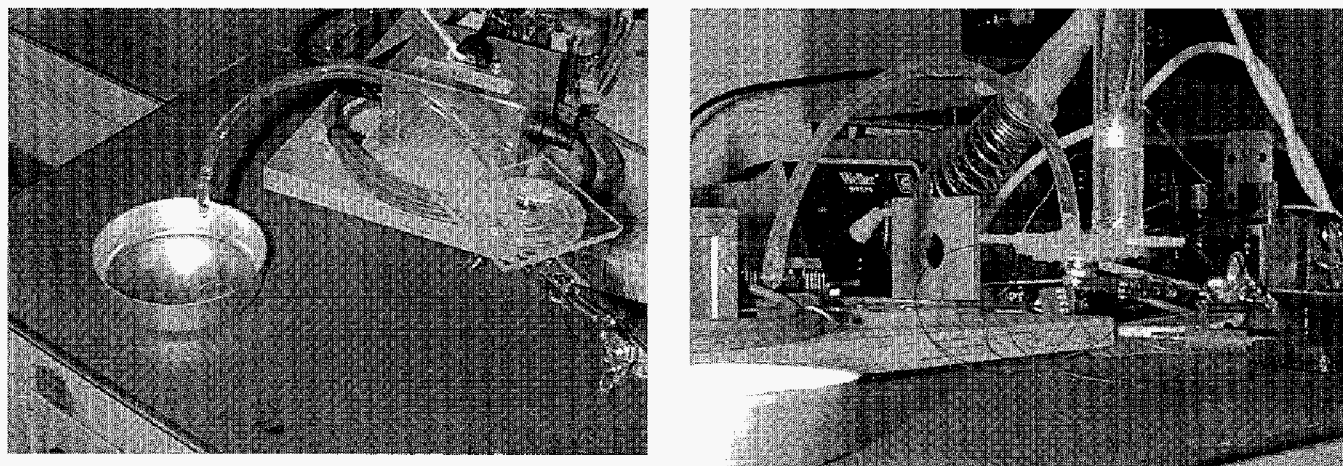

Figure 12: A working pump is pumping water.

5. CONCLUSIONS

A piezopump was developed that is driven by traveling flexure waves providing a novel volume displacing mechanism. A piezoelectric ring was bonded to the stator of the pump to induce elastic waves traveling along the metal ring of the stator. The space between the peaks and valleys of the wave is used to peristaltically move water along the wave. Pump parts were produced, assembled, and tested to demonstrate the feasibility of the novel piezopump concept. Currently, the pump is pumping at the rate of 4.5-cc per minute with the highest-pressure level of 1100 Pascal. More theoretical analysis and tests are conducted to improve the performance of the pump.

REFERENCES

Bar-Cohen Y., X. Bao, and W. Grandia, "Rotary Ultrasonic Motors Actuated By Traveling Flexural Waves," Proceedings of the SPIE International Smart Materials and Structures Conference, SPIE Paper No. 3329-82, San Diego, CA, March 1-6, 1998.

Bar-Cohen Y., and Z. Chang, "Piezoelectrically Actuated Miniature Peristaltic Pump", Proceedings of the SPIE Smart Structures Conference, SPIE Paper No. 3992-102, Newport Beach, CA, March 6-8, 2000.

Hagood W., and A. McFarland, "Modeling of a Piezoelectric Rotary Ultrasonic Motors", SPIE Paper no. 2190E52, Smart Structures and Materials 1994: Smart Structures and Integrated Systems, Nesbitt Hagood, (Ed.), SPIE Proc. Vol. 2190, 1994, pp. 814-828.

Hollerbach I., W Hunter and J Ballantyne, "A Comparative Analysis of Actuator Technologies for Robotics." In Robotics Review 2, MIT Press, Edited by Khatib, Craig and Lozano-Perez (1991).

Hosoe, "An Ultrasonic Motor for Use in Autofocus Lens Assemblies," Techno. May, 1989, pp. 3641 (in Japanese).

Inoue, S. Takahashi and M. Saga, "Application of Ultrasonics to Paper Transport Mechanisms," Techno., (May, 1989) pp. 4749 (in Japanese).

Lih S.-S., and Y. Bar-Cohen "Rotary Piezoelectric Motors Actuated by Traveling Waves," Proceedings of the Smart Structures and Materials Symposium, Enabling Technologies: Smart Structures and Integrated Systems, SPIE 3041, ISBN 0-8194-2454-4, June 1997.

Lucovsky (ed.), "Vacuum mechanics", American Vacuum Society Series, No. 7, Conference Proceedings, No. 192, American Institute of Physics, New York (1989).

"Seiko Ultrasonic Micromotor Data Sheets", Seiko instruments Inc., Precision Instruments Department, Consumer Products Div., 1-9-1 Miyakubo, Ichikawa-shi. Chiba 272 Japan, (1992).

Weissler and R. W. Carlson, "Vacuum Physics and Technology", Academic Press, New York (1979).